



HAL
open science

Activity measurements and determination of nuclear decay data of ^{166}Ho in the MRTDosimetry project

Christophe Bobin, Jacques Bouchard, Vanessa Chisté, S.M. Collins, P. Dryák, A. Fenwick, J. Keightley, Marie-Christine Lépy, Valérie Lourenço, A.P. Robinson, et al.

► To cite this version:

Christophe Bobin, Jacques Bouchard, Vanessa Chisté, S.M. Collins, P. Dryák, et al.. Activity measurements and determination of nuclear decay data of ^{166}Ho in the MRTDosimetry project. Applied Radiation and Isotopes, 2019, 153, pp.108826. 10.1016/j.apradiso.2019.108826 . hal-03433603

HAL Id: hal-03433603

<https://hal.science/hal-03433603v1>

Submitted on 28 Jan 2022

HAL is a multi-disciplinary open access archive for the deposit and dissemination of scientific research documents, whether they are published or not. The documents may come from teaching and research institutions in France or abroad, or from public or private research centers.

L'archive ouverte pluridisciplinaire **HAL**, est destinée au dépôt et à la diffusion de documents scientifiques de niveau recherche, publiés ou non, émanant des établissements d'enseignement et de recherche français ou étrangers, des laboratoires publics ou privés.

Activity measurements and determination of nuclear decay data of ^{166}Ho in the MRTDosimetry project

Bobin^{a*}, C., Bouchard^a, J., Chisté^a, V., Collins^b, S.M., Dryák^c, P., Fenwick^b, A., Keightley^b, J., Lépy^{.a}, M.-C., Lourenço^a, V., Robinson^{b, d, e}, A. P., Sochorová^c, J., Šolc^c, J., Thiam^a, C.

^aCEA, LIST, Laboratoire national Henri Becquerel, (LNE-LNHB), 91191 Gif-sur-Yvette Cedex, France

^bNational Physical Laboratory, Hampton Road, Teddington, Middlesex, TW11 0LW, United Kingdom

^cCzech Metrology Institute, Okružní 31, 638 00 Brno, Czech Republic

^dUniversity of Manchester, Oxford Road, Manchester, M13 9PL, United Kingdom

^eChristie Medical Physics and Engineering (CMPE), The Christie NHS Foundation Trust, Wilmslow Road, M20 4BX, Manchester, United Kingdom

* Corresponding author

e-mail address: christophe.bobin@cea.fr

Keywords

Ho-166, Activity standardization, γ -spectrometry, half-life measurements, molecular radiotherapy, MRTDosimetry project

Abstract

Holmium-166 is a high-energy β^- -emitter radionuclide (~ 1.8 MeV) with a short half-life (~ 26.8 h) that offers great potential as an alternative to ^{90}Y for the treatment of liver cancer based on radioembolization. The possibility of quantitative Single Photon Emission Computed Tomography (SPECT) imaging of the main γ -ray emission at 80.6 keV, in addition to strong paramagnetic properties suitable for Magnetic Resonance Imaging (MRI), complement this therapeutic potential. The present paper describes the measurements carried out in three European radionuclide metrology laboratories for primary standardization of ^{166}Ho and new determinations of X- and γ -ray photon-emission intensities in the framework of the European EMPIR project MRTDosimetry. New half-life measurements were also performed.

Highlights

- Standardization of ^{166}Ho performed using three primary techniques at three NMIs
- Absolute X- and γ -ray intensities determined by γ -ray spectrometry
- Five half-life measurements performed by ionization chamber and gamma-ray spectrometry

1. Introduction

Holmium-166 disintegrates through 100% β^- emission with maximum beta energies of approximately 1.8 MeV ($T_{1/2}$ (^{166}Ho) \sim 26.8 h), that makes it of interest for medical radiotherapeutic applications. In 2015, a new Selective Internal Radiotherapy (SIRT) product based on ^{166}Ho -labelled microspheres (QuiremSpheres®, Quirem Medical BV) was approved for use in Europe for the treatment of liver cancer based on radioembolization. In SIRT, ^{166}Ho -labelled microspheres have been developed as a possible alternative to ^{90}Y -labelled microspheres using the same therapeutic principle. Two types of ^{90}Y -microspheres are currently available in clinics: resin microspheres (SIR-Spheres, Sirtex) and glass microspheres (TheraSphere, BTG). As ^{90}Y is a pure β^- emitter ($E_{\beta\text{max}} \sim 2.3$ MeV; $T_{1/2}$ (^{90}Y) \sim 2.67 d), quantitative imaging applied for patient-specific dosimetry can be implemented by means of either bremsstrahlung SPECT or PET based on the low intensity e^+/e^- internal pair production. Taking advantage of the γ -ray emission following ^{166}Ho disintegration (80.6 keV, $I_\gamma \sim 6.55\%$) for SPECT imaging, the accuracy of image reconstruction can be improved compared to quantitative imaging with ^{90}Y . In addition, multimodality imaging can be implemented by combining magnetic resonance imaging thanks to the paramagnetic property of holmium (Seevinck et al., 2007).

The MRTDosimetry project (Metrology for clinical implementation of dosimetry in molecular radiotherapy) is a Joint Research Project within the European Metrology Programme for Innovation and Research (MRTDosimetry, 2016). It was initiated to bring together expertise in metrology and nuclear medicine research to address the problem of determining the absorbed radiation dose to individual patients who are undergoing molecular radiotherapy (MRT). This therapeutic technique allows the optimization of absorbed dose delivered to a specific target lesion (e.g. tumors), whilst sparing nearby healthy tissue. The project began in June 2016 for three years. As part of the objectives of the MRTDosimetry project, the present article describes the studies carried out in three European radionuclide metrology laboratories: Czech Metrology Institute (CMI), Laboratoire national Henri Becquerel (LNHB) and the National Physical Laboratory (NPL) for the realization of primary standards of ^{166}Ho and new determinations of nuclear data. Measurements of the X- and γ -rays were carried out with the aim to provide new photon emission intensities for inclusion in the evaluated nuclear databases. The current recommended half-life of ^{166}Ho of 26.795 (29) h from the Decay Data Evaluation Project (DDEP) (Bé et al., 2004) is heavily weighted towards

two precise but discrepant measurements published before 1999 (Abzouzi et al., 1989; Unterweger et al., 1992). New measurements were performed by the participating laboratories using different types of instruments (ionization chambers and γ -spectrometers). For the measurements performed within the MRTDosimetry project, a half-life value that had been provisionally evaluated by the DDEP was used. This evaluation incorporated publications up to 2017, with modification to the standard uncertainty of Abzouzi et al. (1989) and using the reported standard uncertainty in Unterweger et al. (2002) over that reported in Unterweger and Fitzgerald (2014). This evaluation provided a $T_{1/2}(^{166}\text{Ho}) = 26.824 (30) \text{ h}$ (Kellet, 2017).

2. Primary measurements and photon-emission intensities in the decay of ^{166}Ho

2.1 Measurements at LNHB

2.1.1 Source preparation

The radioactive solution of ^{166}Ho was obtained from the IAE POLATOM radioisotope center (Poland) and it was received on 25 October 2017. The solvent was 0.1 mol.L^{-1} hydrochloric acid ($\rho = 1.000 \text{ g.cm}^{-3}$). The reference date for all measurements was chosen to be 27 October 2017 at 00:00 UTC to limit decay corrections between measurement methods.

For ^{166}Ho primary standardization, photon-emission intensities and half-life measurements, radioactive sources were prepared from solutions at two nominal activity concentration levels:

- at 8 MBq.g^{-1} : five BIPM ampoules were filled with 3.6 mL of solution for ionization chamber calibration and half-life measurements; standard glass vials filled with 10 mL Hionic Fluor for liquid scintillation measurements based on the Triple-to-Double Coincidence Ratio method (TDCR) (Broda et al., 2007) and point sources on $18 \mu\text{m}$ Mylar® for γ -spectrometry (at least 80 kBq at source preparation time), were prepared;
- at 2 MBq.g^{-1} : gold-coated VYNS solid sources ($\sim 30 \text{ nm Au}$ on both sides) for $4\pi\beta\text{-}\gamma$ coincidence counting (Campion, 1959) were prepared.

Due to the high stable Ho content in the mother solution provided by POLATOM, the excess of stable element was always higher than 15,000 during source preparation and

enabled the stability of the radionuclide in solution. No radioactive impurity was detected by gamma spectrometry.

2.1.2 Primary measurements

2.1.2.1 $4\pi\beta\text{-}\gamma$ coincidence counting

The standardization of the ^{166}Ho radioactive solution at $2\text{ MBq}\cdot\text{g}^{-1}$ using the $4\pi\beta\text{-}\gamma$ coincidence method (Campion, 1959) was carried out using a live-timed anticoincidence system instrumentation (Bobin et al., 2007) based on home-made electronic modules developed at LNHB (Bouchard, 2000; 2002). The measurements of the solid sources was implemented using a detection setup composed of a pill-box proportional counter in the β -channel (filled with CH_4 at atmospheric pressure) coupled to a $44\text{ mm} \times 5\text{ mm}$ $\text{NaI}(\text{Tl})$ detector in the γ -channel. The efficiency-extrapolation technique (Baerg, 1973) was carried out by adding gold-coated VYNS foils on solid sources. Coincidence counting was performed using a γ -window centered on the 80.6 keV -energy peak yielding experimental $\frac{N_c}{N_\gamma}$ ratios ranging between 0.969 and 0.994 (N_c and N_γ respectively represent coincidence and γ -count rates). The activity concentration was assessed from the fitting of experimental data using the classical straight-line function depending on the variable $(1 - \frac{N_c}{N_\gamma})/\frac{N_c}{N_\gamma}$. The analysis of the residuals did not reveal a problem with non-linearity. The high value obtained for the slope (0.47 (2)) is mainly due to the fact that 80.6 keV γ -transition is highly converted. The uncertainty budget is given in Table 1. The main contributions are due to the efficiency-extrapolation technique and the correction for the radioactive decay.

2.1.2.2 Triple-to-Double Coincidence Ratio counting

The radioactive solution at $8\text{ MBq}\cdot\text{g}^{-1}$ was assessed by liquid scintillation counting using the TDCR method. The detection apparatus is based on three XP2020Q photomultipliers (Photonis) coupled to a MAC3 module (Bouchard and Cassette, 2000) which was modified to set variable resolving time for TDCR counting. A resolving time equal to 80 ns was used for the standardization of ^{166}Ho . Due to the high-energy electrons emitted by ^{166}Ho , high TDCR values greater than 0.996 were obtained. For each of the measured sources, the calculation of the detection efficiency of double coincidences was based on the classical free-parameter statistical model (Broda et al., 2007) constructed using the Python programming language. For that purpose, the four main β -branches of ^{166}Ho ($\beta_{0,0}^-$, $\beta_{0,1}^-$, $\beta_{0,4}^-$

and $\beta_{0,6}^-$) and their related probabilities were considered (Bé et al., 2004). The corresponding β -spectra were calculated using the BetaShape code (Mougeot, 2015). Regarding γ -transitions, only the highly-converted 80.6-keV transition was taken into account in the analytical modelling. The related distribution of deposited energy in the scintillation cocktail (Hionic Fluor) by Compton diffusion was determined by Monte Carlo calculations using the Geant4 simulation toolkit (Agostinelli et al., 2003; Bobin et al., 2016). The activities of the five LS sources were calculated using a kB value equal to 0.01 cm.MeV^{-1} . The uncertainty budget is given in Table 2. Both results given by TDCR counting and $4\pi\beta$ - γ coincidence (taking in account the dilution factor) at the reference date are in good agreement within their respective uncertainties.

2.1.3 Photon spectrometry

The measurements of photon emission intensities were performed from four point sources with masses ranging from 9.7 mg to 30 mg, prepared from the 8 MBq.g^{-1} solution. First, a homogeneity check was carried out, and showed that it was necessary to take into account a relative uncertainty of 0.7% related to the representativeness of these sources. The subsequent measurements were carried out using three high-purity germanium (HPGe) detectors, two coaxial and one planar, to better cover the range of photon energies and ensure the consistency of the results.

2.1.3.1 High-energy spectrometry

Two 100 cm^3 coaxial HPGe detectors were calibrated over the energy range from 15 keV to 1836 keV using point sources prepared from LNHB standard solutions whose activity is known with relative uncertainty of a few per thousands. The source-to-detector window (calibration position) distance is approximately 10 cm (see Table 3).

For each detector, more than eighty experimental values (energy, E_i , full-energy peak (FEP) efficiency, ε_i) were obtained with: ^{22}Na , ^{51}Cr , ^{54}Mn , ^{57}Co , ^{58}Co , ^{60}Co , ^{59}Fe , ^{65}Zn , ^{85}Sr , ^{88}Y , ^{109}Cd , ^{131}I , ^{133}Ba , ^{134}Cs , ^{137}Cs , ^{139}Ce , ^{152}Eu , ^{207}Bi , ^{210}Pb , ^{241}Am . Coincidence-summing corrections are taken into account, and the maximum correction factors are 1.03 for the multigamma-emitting radionuclides. The overall FEP efficiency curve is obtained by adjusting a log-log polynomial to the experimental data. The associated relative uncertainties are in the order of 0.5% to 1%.

The photon-emission intensities for each energy E_i , I_i , are derived as the average of the individual results obtained from the measurement of three sources, as:

$$I_i = \frac{N_i \cdot C_T \cdot C_D \cdot C_G \cdot C_{Ci}}{A \cdot \varepsilon_i \cdot t} \quad (1)$$

where N_i is from the net counting in the full-energy peak, obtained using GAMMAVISION® (ORTEC, 2018) for well isolated peaks or COLEGRAM (Ruellan et al., 1996) for the complex regions. A is the source activity (Bq) determined from the primary measurement and t is the measurement live time. The FEP efficiency, ε_i , is obtained from the calibration procedure. Corrections for the radionuclide decay, C_T and C_D are respectively computed to account for the radioactive decay between the reference date and acquisition start time and the decay during the measurement. Corrections for source geometry, C_G , and coincidence summing effects, C_{Ci} , are computed using ETNA software (Piton et al., 2000). For the measurements in the calibration conditions, C_G , is 1.0 and C_{Ci} is less than 1.01.

In order to obtain experimental values for the low intensity lines, complementary measurements were carried out with a short source-detector distance (2 cm) and by interposing a 1.96 mm-thick lead screen to attenuate bremsstrahlung and thus improve detection limits. However this technique introduces a strong efficiency transfer factor (5 to 6) and, consequently, higher uncertainties associated with the photon emission intensities determined. A relative uncertainty of 5% was initially introduced for the efficiency transfer factor component; however, given the good agreement between the results obtained with and without transfer correction, this uncertainty value was reduced to 2%.

Table 4 presents the absolute photon emission intensities obtained in the calibration condition and at 2 cm with a screen. These are respectively obtained with 1.3% to 2.6% and 2.4% to 5.3% relative combined uncertainties.

2.1.3.2 Low-energy spectrometry

Additional measurements were made on a planar HPGe detector to confirm the emission intensity of the 80.6-keV line and to determine the individual components of the K X-rays emissions. As with the coaxial detectors, three sources were measured at the calibration position, at 8 cm from the detector window. The FEP efficiency calibration was performed over the energy range from 12 keV to 180 keV, with standard radioactive sources (^{57}Co , ^{88}Y , ^{109}Cd , ^{133}Ba , ^{137}Cs , ^{139}Ce , ^{152}Eu , ^{241}Am) providing about forty experimental values

(E_i, ε_i). The overall FEP efficiency curve was obtained by adjusting a log-log polynomial to these values. The associated relative standard uncertainties are in the order of 1%. By following the same process as for the high-energy range, the low-energy photon emission intensities are derived as the average of the individual results obtained from the measurement of three sources, according to equation (1). It can be noted that the K X-ray energy region was processed using COLEGRAM, using a Voigt function to fit the experimental data, taking into account the natural width of X-rays (Campbell and Papp., 2001); an example of the Voigt functions fitting in the X-ray region is presented in Fig. 1.

The resulting photon emission intensities are quoted in Table 5; they are obtained with relative combined uncertainties ranging from 1.1% to 3.1%.

2.1.3.3 LNHB results

Table 6 summarizes the absolute photon-emission intensities in the decay of ^{166}Ho measured at LNHB, compared with the DDEP values. The different results for the emission intensity at 80.6 keV are used to compute the final value as the weighted average of five compatible results, *i.e.* 6.61 (7), which is in good agreement with the DDEP values. The associated uncertainty budget is given in Table 7. The intensities of the other gamma emissions are taken from Table 4, column 2 for the main emissions and column 3 for the lower intensities which were obtained out of the calibration conditions. For the K X-ray emissions, the results provided by the planar detector (see Table 5) are kept because this detector has been calibrated in details in the energy range below 60 keV and has a better resolution than the larger detectors.

This series of measurements allowed the determination of nine absolute gamma emission intensities for ^{166}Ho : these results are obtained with standard uncertainties ranging from 1.3% to 5.3% and are in good agreement with the recommended values from DDEP (Bé et al., 2004). However, the measured emission intensities of K X-rays are significantly higher than the DDEP values, by about 4% for K-alpha and 12% for K-beta. Further investigations would be required to confirm this deviation, which raises the difficulties of FEP calibration at energies below 80.6 keV due to the lack of absolute references (Lépy et al., 2018).

2.2 Measurements at CMI

2.2.1 Primary measurements

The standardization of ^{166}Ho at CMI was performed using the $4\pi\beta\text{-}\gamma$ coincidence method (Campion, 1959) and the efficiency-extrapolation technique (Baerg, 1973). The detection system consists of a stainless-steel cylindrical proportional counter (dimensions: 2 x (height: 18 mm, diameter: 64 mm)) operating with methane at atmospheric pressure in a gas flow arrangement. The γ -ray detection assembly is composed of two opposing NaI(Tl) detectors. For coincidence counting, a γ -window centered on the 80.6 keV-energy peak was applied.

For source preparation, the radioactive solution was prepared from an original solution (15.9 $\mu\text{g}\cdot\text{g}^{-1}$ $\text{Ho}(\text{NO}_3)_3$ in a 1 M solution of HNO_3) diluted so that its nominal activity at the reference time was 300 $\text{kBq}\cdot\text{g}^{-1}$. For coincidence counting, fifteen solid sources were prepared by deposition of 20-50 mg aliquots of diluted solution onto gold-coated VYNS films ($\sim 40 \mu\text{g}\cdot\text{cm}^{-2}$) treated with Ludox and insulin. Gold-coated VYNS foils were also used to cover solid sources in order to decrease the detection efficiency in the β -channel for the application of the efficiency-extrapolation technique. Analysis of data obtained by measurement of samples covered by various number of additional foils confirmed the expected extrapolation linearity for $\frac{N_\beta N_\gamma}{N_c}$ as a function of $(1 - \frac{N_c}{N_\gamma}) / \frac{N_c}{N_\gamma}$, where N_β , N_γ and N_c are corrected count rates according to Smith (1987). The resulting activity concentration was determined from the extrapolation with $\frac{N_c}{N_\gamma}$ in the range of 0.98 – 0.995. The normalized extrapolation slope was 0.473(18). The uncertainty budget is given in Table 8.

2.2.2 Measurements of photon-emission intensities

Photon-spectrometry measurements were carried out at CMI using three spectrometric systems manufactured by Canberra:

- System one: HPGe detector, named GCX, energy resolution equal to 1.8 keV at 1332 keV, relative detection efficiency 41%, preamplifier 2002CSL, connected to a MCA LYNX.
- System two: HPGe detector, named GC4018, energy resolution equal to 1.8 keV at 1332 keV, relative efficiency 40%, preamplifier 2002CSL, connected to a MCA LYNX.
- System three: HPGe detector type BEGe, energy resolution equal to 1.9 keV at 1332 keV, relative detection efficiency 48%, entrance window Carbon Epoxy, preamplifier 2002CSL, connected to MCA LYNX.

As shown in Fig. 2, the BEGe system presents a weak dependence of the detection efficiency on photon energy in the region from 20 to 130 keV. Dead-time and pile-up effect corrections were made electronically. They were smaller than 0.5% in all the measurements. For the three systems, detection efficiencies were calculated by a Monte Carlo (MC) method using the code MCNP (Briesmeister, 2000). The MC method was validated by comparing MC simulations and measurements for the distances of 26 cm (GCX) and 25 cm (GC4018 and BEGe) (Dryák and Kovář, 2006).

From the original non-diluted solution of ^{166}Ho , two sources of the EFS-type (Eurostandard CZ) were prepared. The activity (3 MBq at the reference date) was deposited between two welded polyethylene (PE) foils (thickness: 0.2 mm). Each source was measured using the three spectrometric systems and placed at the same source-to-detector distance used for calibration. A total of six or nine spectra for each combination of detector-source were recorded. For each measurement, the live time was set to 1000 s.

The dead time of the GC4018 and GCX detectors varied between 0.8% and 1.9%, but reached values ranging between 5.8% up to 12.1% in the case of the BEGe detector due to the detection of beta radiation. Therefore, the pile-up correction for the BEGe measurements has a higher uncertainty. Measurements with the BEGe detector also had to be corrected for coincidence summing effect reaching 0.206% due to coincidences with beta radiation (maximum energy of $E_{\text{max}} = 1774$ keV). The same correction for the measurements with GCX and GC4018 detectors was only 0.001%.

The photon-emission intensity at 80.6 keV was determined from the measurements obtained with the three spectrometric systems using an equation similar to Eq. (1). The combined value from each result (see Table 9) was equal to 6.636 with a relative uncertainty of 0.74%. The uncertainty budget for the 80.6 keV photon emission intensity is given in Table 7.

The coincidence summing effects of 80.6 keV and K X-ray photons with high-energy beta radiation ($E_{\text{max}} = 1774$ keV) is not negligible in measurements with the BEGe detector. Coincidence probability is equal to 98%. The total detection efficiency for beta particles with emission spectrum was determined by means of MC simulations for an EFS source at the distance of 25 cm from the BEGe detector. The total detection efficiency is $2.100(36) \times 10^{-3}$ yielding a correction of 1.0021. In addition, measurement with the BEGe detector has also to be corrected for the coincidence summing effects of 1379 keV and 1581 keV photons with

80.6 keV or K X-ray photons with the 100% coincidence probability. The total detection efficiency for both 80.6 keV and KX photons is 0.56%, therefore the correction equals to 1.0056.

The 1379 keV, 1581 keV, and 1662 keV photon peak areas were determined using the CANBERRA GENIE 2000 software. The K X-ray peak areas were also determined by the software. K_{α} and K_{β} doublets were fitted with the double Gaussian curves with a linear background. The absolute photon-emission intensities of ^{166}Ho determined at CMI are reported in Table 6.

2.3 Measurements at NPL

2.3.1. Source preparation

A supply of ^{166}Ho , as an aqueous solution in 1 M HCl with $10 \mu\text{g.g}^{-1}$ inactive Ho carrier, was delivered to NPL from Quirem Medical B.V. at a nominal activity of 339 MBq.g^{-1} at 2018-05-24 12:00 UTC. The supplied solution was diluted with 1 M HCl with $10 \mu\text{g.g}^{-1}$ inactive Ho carrier to produce a solution with a nominal activity of 10.5 MBq.g^{-1} . From this solution 1 g aliquots were dispensed to two 2 mL ISO glass ampoules for photon emission intensity measurements.

Due to the 26.8 h half-life, to minimise time taken to prepare the samples it was decided to forego the radiometric validation of the gravimetric dilution of the solution. Instead, two separate gravimetric dilutions were made and the self-consistency in their activities used to confirm the gravimetric dilution. Two portions of the solution were taken and gravimetrically diluted using 1 M HCl with $10 \mu\text{g.g}^{-1}$ inactive Ho carrier, to provide two solutions (DIL1 and DIL2) with respective nominal activities of 120 kBq.g^{-1} and 100 kBq.g^{-1} . These solutions were used to prepare two further sets of six plastic LS vials, containing aliquots of 150 mg (DIL1) and 100 mg (DIL2) of the solution in 10 mL of Gold Star Quanta liquid scintillant and 0.1 mL of 1 M HCl with $10 \mu\text{g.g}^{-1}$ inactive Ho carrier.

2.3.2. Radionuclide contaminants

The presence of any γ -ray emitting radionuclide impurities was investigated by HPGe γ -ray spectrometry, specifically the long-lived $^{166\text{m}}\text{Ho}$. The solutions were measured at the earliest opportunity to determine if any short-lived radionuclides were present, and then later when the ^{166}Ho had decayed through at least twenty half-lives. No short-lived radionuclide impurities were detected but $^{166\text{m}}\text{Ho}$ was found. The solution was found to contain

30 (12) Bq.g⁻¹ at the reference time of 2018-05-24 12:00 UTC, or a $A_0(^{166\text{m}}\text{Ho})/A_0(^{166}\text{Ho})$ ratio of 0.00032%.

2.3.3 Primary standardization by 4π(LS)-γ Digital Coincidence Counting

2.3.3.1. Experimental setup

The NPL 4π(LS)-γ digital coincidence counting (DCC) system was used to measure all the prepared LS vials and the subsequent pulse trains were captured, digitized and stored in the NPL list mode format. The detector system and the DCC system for data processing has previously been described in Keightley et al. (2015). The coincidences were formed using the LS channel and the γ-gate set on the 80.6 keV γ ray emitted from the 2⁺ → 0⁺ transition from the 80.6 keV excited level (ΔT = 1.82 ns) of ¹⁶⁶Er. This transition is highly converted (α_T = 6.9) and thus there are significant X-rays emitted between 48 keV – 58 keV. The efficiency extrapolation was performed using the function:

$$\frac{N_\beta}{\varepsilon_\beta} = N_0 + a_1 \left(\frac{1}{\varepsilon_\beta} - 1 \right) + a_2 \left(\frac{1}{\varepsilon_\beta} - 1 \right)^2 \quad (2)$$

2.3.3.2 Results

The DIL1 and DIL2 sets of vials were each measured once on the 25 May 2018. The activity per unit mass of each diluted solution was determined from the arithmetic mean of these measurements, decay corrected to the reference time of 12:00 UTC on the 25 May 2018, using the half-life of 26.824 h. Accounting for the gravimetric dilution factor for each diluted solution, the activity per unit mass of the starting solution was determined from the arithmetic mean of the combined DIL1 and DIL2 measurements. An activity per unit mass of 9.481 (41) MBq g⁻¹ at the reference time of 12:00 UTC on the 24 May 2018 was determined. The uncertainty budget is given in Table 10.

The relative difference between the activities determined from the DIL1 and the DIL2 vials was 0.28%. This relative difference is not statistically significant considering the relative standard deviation of each of the two set of vials (ξ-score = 0.78). This indicates that there were no observable complications in the gravimetric dilutions.

2.3.4 Measurement of the photon-emission intensities

The photon-emission intensities were determined using the two samples prepared in section 2.3.1., with each sample measured three times over the course of two days. The measurement periods varied from 3 400 s to 60 000 s, the longer counting times allowed for the detection and improved statistics for the small intensity emissions relative to the 80.6 keV emission. These samples were measured using the same HPGe γ -ray spectrometer system and FEP efficiency calibration detailed in Collins et al. (2018). The same process to calculate the emission intensities as described in Collins et al. (2018) was used.

The absolute emission intensities determined at NPL are presented in Table 6. The uncertainty budget for the absolute emission intensity of the 80.6 keV γ -ray is given in Table 7. A total of ten gamma-ray emissions were detected and their emission intensities quantified. The detection limits of the HPGe gamma-ray spectrometer were not sufficient that the remaining seven gamma-ray emissions in the currently proposed ^{166}Ho decay scheme could be quantified. The quoted gamma-ray intensities are typically in agreement with those recommended by the DDEP (Bé et al., 2004), with improvements in the precision over them.

As detailed in section 2.3.2., the presence of $^{166\text{m}}\text{Ho}$ was identified, which shares several of the characteristic γ -ray emissions that occur from the decay of ^{166}Ho ; specifically, the 80.6 keV and 184.4 keV γ rays. Corrections for these interferences were applied to these net peak areas, using the recommended DDEP nuclear data (Bé et al., 2004). While this correction is insignificant in most cases, where the corrections were typically less than 0.0008%, it has a significant impact on the 184.4 keV full-energy peak due to the ratio of the emission intensities from the ^{166}Ho and the metastable state ($I_{\gamma}(^{166\text{m}}\text{Ho})/I_{\gamma}(^{166}\text{Ho}) \sim 52\,000$). The $A_t(^{166}\text{Ho})/A_t(^{166\text{m}}\text{Ho})$ ratio of the full-energy peak area contribution for the initial measurement was approximately 16%, rising to approximately 59% by the final measurement due to the rapid decay of the ^{166}Ho and the long-lived nature of $^{166\text{m}}\text{Ho}$.

Considering the 184.4 keV emission more closely, the underlying normalised values that have been used to derive the recommended value show a significant discrepancy (ξ -score = 9.2) between the two most precise values of Chand et al. (1989) and Ardisson et al. (1992). The addition of the NPL value does not provide a resolution to this disagreement, favouring neither of these two reported values and quoting a standard uncertainty that is approximately the same magnitude. Further measurements are required to resolve the observed discrepancy in this dataset.

3. Half-life measurements of ^{166}Ho

3.1 Measurements at LNE-LNHB

3.1.1 Ionization chamber (Vinten type 671 IC)

The measurement of the ^{166}Ho half-life based on the Vinten type 671 IC (N_2 at a pressure of 10 MPa) was performed using a BIPM ampoule filled with 3.6 mL of radioactive solution. Current measurements were carried out every hour using a Keithley 6517A electrometer. Each value was obtained from the estimation of a slope of 50 voltage samples acquired every 2 s. A total of 300 current measurements were recorded over a period corresponding to more than 11 half-lives of ^{166}Ho . The experimental values were ranged between 2.75 pA and 2×10^{-2} pA (corresponding to approximately to the background level). No geometry change on the BIPM ampoule positioning was performed during the whole measurement.

A nonlinear fitting analysis based on the Levenberg-Marquardt algorithm was first applied to the 300 current measurements using the basic decay function (3) depending on the half-life $T_{1/2}$ and the background level B_k .

$$C(t) = C_0 \times e^{-\frac{\ln(2) \times t}{T_{1/2}}} + B_k \quad (3)$$

The results of the fitting were respectively $T_{1/2}$ equal to 26.804 (11) h and B_k equal to $1.95 (3) \times 10^{-2}$ pA. The agreement of the latter value with the experimental background was interpreted as a good indicator that no significant drift occurred during the measurement period. The relative residuals are plotted in Fig. 3. It is worth noting that the last half of the residuals clearly show large variabilities corresponding to low-level measurements close to the background. In consequence, a new fitting analysis was applied by only considering the first 120 current measurements using a background level equal to 1.95×10^{-2} pA. In that case, the resulting half-life $T_{1/2}$ of ^{166}Ho was equal to 26.806 (12) h.

The uncertainty was reassessed taking into account the recommendations given in Pommé (2015) and applied in recent articles such as D'Agostino et al. (2017). Basically, it is suggested to consider three types of frequencies for the uncertainty components: high- (statistics), medium- (cyclic) and low-frequency (drift) deviations. The statistics component (0.05%) was determined using the standard deviation of the relative residuals of the first 120 current measurements (~ 4.5 half-lives) as described in Pommé (2015). The medium-frequency component (0.03%) was assessed using the standard deviation of the estimated half-lives obtained by adding successively twelve current measurements in the fitting analysis.

The low-frequency contribution (0.03%) was obtained by variation of the background level. Finally, a half-life $T_{1/2}$ equal to 26.806 (18) was obtained from the decay measurements of the Vinten type 671 IC (the uncertainty budget is given in Table 11)

3.1.2 Gamma counting using a NaI(Tl) detector

The measurement of the ^{166}Ho half-life based on γ -counting were carried out by means of the detection set-up dedicated to $4\pi\beta\text{-}\gamma$ coincidence counting using a solid source placed in the proportional counter. The counting was performed using a NaI(Tl) detector (44 mm (diameter) \times 5 mm (height)) at a distance of about 5 cm from the radioactive source and surrounded by a lead shielding. The detection set-up was installed in a temperature-stabilized area. A total of about 230 γ -spectrum measurements (acquisition duration equal to 1800 s) were recorded every hour corresponding to more than eight half-lives of ^{166}Ho . The dead-time management was implemented using a home-made module (Bouchard, 2000) based on the live-time technique and extendable dead-time. Each γ -counting was determined using a γ -window comprising the main photon emissions of ^{166}Ho (X_L , X_K and γ at 80.6 keV). Using this setting, the γ -counting was ranged between $132.0 (3) \text{ s}^{-1}$ and $0.67 (2) \text{ s}^{-1}$ and the background level was equal to $0.35 (2) \text{ s}^{-1}$.

The fitting analysis was applied on the whole measurement using the decay function (3) and by letting the background variable as free. In that condition, the half-life $T_{1/2}$ was equal to 26.818 (16) h and the calculated background ($0.37 (2) \text{ s}^{-1}$) was in agreement with the experimental value. The relative residuals displayed in Fig. 4 do not show a significant trend. The uncertainty was reassessed according to the recommendations given in Pommé (2015). The statistics component (0.05%) was determined using the standard deviation of the relative residuals of the 230 current measurements. The medium- (0.03%) and low-frequency components (respectively 0.03% and 0.05%) were determined in the same manner as for IC measurements. Finally, a half-life $T_{1/2}$ equal to 26.818 (21) was obtained from γ -counting using a solid source. The associated uncertainty budget is given in Table 12. This value is in good agreement with the half-life determined using the Vinten type 671 IC results.

3.2 Measurements at CMI

The radioactive sources prepared for the measurement of photon-emission intensities were used for the measurement of the ^{166}Ho half-life with the GCX detector. The measurement geometry was chosen in such a way to keep the dead time below 3.5%. The measured peak area (80.6 keV) was corrected for the decay during the measurement and for

the decay during the dead time. The half-life was estimated from the fitting of the corrected peak area as an exponential function of the time elapsed from the measurement start (the relative residuals are displayed in Fig. 5). A half-life value equal to 26.828 (28) h was obtained. The associated uncertainty budget is displayed in Table 13.

3.3 Measurements at NPL

3.3.1. Ionisation chamber

The NPL secondary standard ionisation chamber, known as the PA782, was used to measure the decay of the ^{166}Ho using the solution described in section 2.3.1. This system has been described in previous half-life determinations (Collins et al., 2015a; 2015b).

The radioactive source was placed in the well of the PA782 and measurements made over 2.76 d. A total of 9051 measurements each of a 25 s period were made. Each data point was background corrected, where the $\text{pA}(\text{Background})/\text{pA}(\text{Observed})$ was 0.029% at the start and 0.16% at the end. To determine the half-life of the ^{166}Ho a non-linear least squares fit was made to the dataset, with two exponential decay functions used to account for the presence of both ^{166}Ho and $^{166\text{m}}\text{Ho}$, using the formula:

$$\text{pA}_t = \text{pA}_0(^{166}\text{Ho}) \cdot e^{-\lambda_{166}t} + \text{pA}_0(^{166\text{m}}\text{Ho}) \cdot e^{-\lambda_{166\text{m}}t} \quad (4)$$

where pA_t is the sum of the currents from ^{166}Ho and $^{166\text{m}}\text{Ho}$ at time t , $\text{pA}_0(^{166}\text{Ho})$ and $\text{pA}_0(^{166\text{m}}\text{Ho})$ the current at t_0 , λ_{166} and $\lambda_{166\text{m}}$ the decay constants of ^{166}Ho and $^{166\text{m}}\text{Ho}$.

The parameters $\text{pA}_0(^{166}\text{Ho})$, $\text{pA}_0(^{166\text{m}}\text{Ho})$ and λ_{166} were incrementally varied while $\lambda_{166\text{m}}$ was fixed using a $T_{1/2}$ of 1133 a (Bé et al., 2004). Through this procedure a $T_{1/2}(^{166}\text{Ho}) = 26.793$ (27) h was determined. The residuals of the least squares fit are shown in Fig. 6a. The uncertainty of the half-life value was derived accounting for the high, medium and low frequency components and deriving the $u(T_{1/2})/T_{1/2}$ for each component using the propagation formula derived by Pommé (2015). The uncertainty budget is presented in Table 14; this does not include any medium frequency components as none were identified during the analysis.

The $^{166\text{m}}\text{Ho}$ impurity was found to be the largest contributor to the combined uncertainty as its higher energy γ rays have a significantly larger response in the ionisation chamber. The calibration factor (CF) for $^{166\text{m}}\text{Ho}$ is approximately 66 pA MBq^{-1} , whereas the ^{166}Ho CF was determined to be approximately 1.3 pA MBq^{-1} ($\text{CF}(^{166\text{m}}\text{Ho})/\text{CF}(^{166}\text{Ho}) \sim 51$).

Therefore, even at low activity ratios the presence of the ^{166m}Ho can have a significant impact on the overall response measured.

3.3.2. High Purity Germanium γ -ray spectrometry

A further solution of ^{166}Ho in 1 M HNO_3 with $10 \mu\text{g}\cdot\text{g}^{-1}$ of stable Ho carrier was supplied to NPL as part of a EUROMET comparison exercise, which had a nominal starting activity of $2 \text{ MBq}\cdot\text{g}^{-1}$ at the reference time of 12:00 UTC on 1 December 2018. This solution was used to prepare a 2 mL ISO ampoule containing an aliquot of 0.20 g of the active solution, which was made up to 1 g with the addition of further 1 M HNO_3 .

The detector described in section 2.3.3. was used to determine the half-life by following the decay rate of the 80.6 keV full-energy peak. A total of 51 measurements were made of the sample over the course of 6.4 d, with a gap of approximately 1 d due to an issue with PC controlling the spectrum collection. The measurements for the initial 4.6 d had a collection time of 7 200 s, this was increased for the following 1 d to 14 400 s, and the final measurements within the campaign period for 20 000 s.

The count rate (s^{-1}) of the 80.6 keV full-energy peak was determined for each spectrum. As with the Ionisation Chamber half-life determination, a non-linear weighted least squares fit was made to the observed count rate (s^{-1}) for each measurement, using the formula:

$$R_t = R_0(^{166}\text{Ho}) \cdot e^{-\lambda_{166}t} \cdot \frac{1-e^{-\Delta t\lambda_{166}}}{\Delta t\lambda_{166}} + R_0(^{166m}\text{Ho}) \cdot e^{-\lambda_{166m}t} \cdot \frac{1-e^{-\Delta t\lambda_{166m}}}{\Delta t\lambda_{166m}} \quad (5)$$

where R_t is the sum of the ^{166}Ho and ^{166m}Ho at time t , $R_0(^{166}\text{Ho})$ and $R_0(^{166m}\text{Ho})$ the count rates of ^{166}Ho and ^{166m}Ho at the reference time. As the measurement time varied throughout the measurement campaign the count rates required decay correction accounting for the decay during measurement, this was performed using the term $\frac{1-e^{-\Delta t\lambda_{166}}}{\Delta t\lambda_{166}}$.

Through the incremental variation of the $R_0(^{166}\text{Ho})$, $R_0(^{166m}\text{Ho})$ and λ_{166} a maximum-likelihood estimate of the count rates and decay constant was determined. A result of $T_{1/2}(^{166}\text{Ho}) = 26.800 (26) \text{ h}$ was determined. The residuals of the least squares fit are shown in Fig. 6b. The major components of the uncertainty budget for the HPGe technique were the dead time, pulse pile up and the continuum fitting (see Table 14).

Consideration of the impact for the 24 h gap in the measurements was made by 1) removing the all the data points prior to the measurement gap (which would have the most

significant impact) and 2) removing the 24 h of data points after the measurement gap. For approach 1) and 2) a change in the half-life value of 0.030% and 0.0075% was observed respectively. These values were not significant within the quoted standard uncertainty. The magnitude of the half-life change due to 1) of approximately 0.03% was covered by the increase of the combined standard uncertainty from 0.10% to 0.14%, due to the measurement campaign being shortened by 1.8 d. Therefore, the effect on the accuracy of the reported half-life due to the measurement gap was considered to be negligible.

Unlike with the ionisation chamber measurement the presence of the $^{166\text{m}}\text{Ho}$ had no observable impact on the observed count rates, even after 6 d. This was due to the ratio of the γ -ray intensities for the 80.6 keV being significantly smaller ($I_{\gamma}(^{166\text{m}}\text{Ho})/I_{\gamma}(^{166}\text{Ho}) \sim 2$) than for the calibration factors on the ionisation chamber for the two radionuclides. By the final measurement of the campaign the $^{166\text{m}}\text{Ho}$ activity was still less than 0.030% of the ^{166}Ho activity, and therefore account for only 0.060% of the count rate.

4 Discussion

Based on independent measurements, primary standardization and new determinations of nuclear data of ^{166}Ho were carried out in three European radionuclide laboratories (CMI, LNHB, NPL) in the framework of the EMPIR project MRTDosimetry. Primary measurements were performed by means of different methods: TDCR method, $4\pi\beta\text{-}\gamma$ and $4\pi(\text{LS})\text{-}\gamma$ coincidence counting using solid and liquid scintillation sources. Because ^{166}Ho is a high-energy β^- -emitter radionuclide (~ 1.8 MeV), high detection efficiencies were obtained in proportional counters or TDCR apparatus leading to low uncertainties associated to the activity concentrations ($\sim 0.2\%$ - 0.4%).

The absolute photon-emission intensity at 80.6 keV used for SPECT imaging, was measured using different γ -spectrometry systems at CMI, LNHB and NPL. The final values presented by CMI and LNHB in Table 6 have been determined from the weighted mean of the results determined by the different detector systems used. The results of the 80.6 keV emission intensities for the three participants are in agreement within the uncertainties. The values quoted in this work have a relative difference of approximately 1% over the currently recommended value from the DDEP but are consistent. A significant difference was obtained between X-ray emission intensities determined at LNHB and those by CMI and NPL. The results from CMI and NPL agree with the recommended values from DDEP (Bé et al., 2004).

It should be noted that CMI and NPL used Gaussian functions to fit the Voight distribution of the X-rays. This will likely have some impact on the accuracy of the values. Further investigations are required to confirm or not this deviation, which raises the difficulties of FEP calibration at energies below 80.6 keV due to the lack of absolute references (Lépy et al., 2018).

Five independent half-life measurements were also carried out at CMI (1), LNHB (2) and NPL (2) using ionization chambers and γ -spectrometers. The two values reported by NPL could be considered completely independent due to different solutions being used on the two detector systems. The results summarized in Table 15 are in agreement. These five half-life measurements are all in agreement, with the current DDEP recommended value of 26.795 (29) h (Bé et al., 2004). They are also in agreement with the re-evaluated half-life used in this MRTDosimetry project.

5 Conclusion

Under the auspices of the MRTDosimetry collaborative project standardizations of the medical radionuclide ^{166}Ho have been performed by CMI, LNHB and NPL. Three independent techniques were used: TDCR, $4\pi\beta$ - γ and $4\pi(\text{LS})$ - γ coincidence counting. Standard uncertainties between 0.2% and 0.4% were achieved. The three participants used these standardized solutions to determine new precise absolute intensities for ten of the 17 proposed photon emissions. The values determined in this work were typically in internal agreement and with those of the DDEP, with the standard uncertainties bettering those of the currently recommended values by the DDEP (Bé et al., 2004). The three 80.6 keV absolute intensity values determined in this work showed a relative increase of approximately 1% over the current recommended value. A total of five half-life measurements were reported by CMI (1), LNHB (2) and NPL (2), using ionization chambers and γ -ray spectrometry. The values reported were consistent internally and with the current recommended value of the DDEP (Bé et al., 2004).

Acknowledgements

The NPL authors would like to thank Quirem Medical B.V. for the supply of ^{166}Ho used for the standardisation and gamma-ray emissions section of their contribution. This work was supported by the European Metrology Programme for Innovation and Research (EMPIR) joint research project 15HLT06 “Metrology for clinical implementation of dosimetry in

molecular radiotherapy” (MRTDosimetry; <http://mrtdosimetry-empir.eu/>) which has received funding from the European Union. The EMPIR initiative is co-funded by the European Union’s Horizon 2020 research and innovation programme and the EMPIR Participating States.

References

Abzouzi, A., Antony, M.S., Ndocko Ndongué, 1989. Precision measurements of the half-lives of nuclides. *J. Radioanal. Chem. Letters.*, 1, 1-7.

Agostinelli, S., Alliso, J., Amako, K., et al., 2003. Geant4 – a simulation toolkit. *Nucl. Instrum. Methods A* 506, 250-303.

Ardisson, C., Barci, V., Dalmaso, J., Hachem, A., Ardisson, G., 1992. Intrinsic and collective ^{166}Er levels fed in the decays of $^{166}\text{Ho}^m$ ($T_{1/2}=1200$ y) and $^{166}\text{Ho}^g$ ($T_{1/2}=26.8$ h). *II Nuevo Cimento* 105, 215-232.

Baerg, A.P., 1973. The efficiency extrapolation method in coincidence counting. *Nucl. Instrum. Methods* 112, 143-150.

Bé, M.M., Chisté, V., Dulieu, C., Browne, E., Chechev, V.P., Kuzmenko, N., Helmer, R., Nichols, A.L., Schönfeld, E., Dersch, R., 2004. Monographie BIPM-5, Table of Radionuclides, ISBN 92-822-2207-1 (Vol. 2). Bureau International des Poids et Mesures, Sèvres, France.

Bobin, C., Bouchard, J., Hamon, C., Iroulart, M.G., Plagnard, J., 2007. Standardization of ^{67}Ga using a $4\pi(\text{LS})\beta\text{-}\gamma$ anti-coincidence system. *Appl. Radiat. Isot.* 68, 757-763.

Bobin, C., Thiam, C., Bouchard, J., 2016. Calculation of extrapolation curves in the $4\pi(\text{LS})\beta\text{-}\gamma$ coincidence technique with the Monte Carlo code Geant4. *Appl. Radiat. Isot.* 109, 319-324.

Bouchard, J., 2000. MTR2: A discriminator and dead-time module used in counting systems. *Appl. Radiat. Isot.* 52, 441-446.

Bouchard, J., Cassette, P., 2002. MAC3: an electronic module for the processing of pulses delivered by a three photomultiplier liquid scintillation counting system. *Appl. Radiat. Isot.* 52. 669-672.

Bouchard, J., 2002. A new set of electronic modules (NIM standard) for a coincidence system using pulse mixing method. *Appl. Radiat. Isot.* 56, 269-273.

Breismeister, J.F., 2000. "MCNP : a General Monte Carlo N-particle Transport code"

Broda, R., Cassette, P., Kossert, K., 2007. Radionuclide metrology using liquid scintillation counting. *Metrologia* 44, S36-S52.

Campbell, J.L, Papp, T., 2001. Widths of the atomic K-N7 levels. *Atomic Data and Nuclear data Tables*, 77(1), 1-56.

Campion, P.J., 1959. The standardization of radioisotopes by the beta-gamma coincidence method using high efficiency detectors. *Int. J. Appl. Radiat. Isot.* 4, 232-248.

Chand, B., Goswamy, J., Mehta, D., Singh, N., Trehan, P.N., 1989. X-ray and gamma-ray intensity measurements in ^{131}I , ^{166}Ho , ^{198}Au and ^{199}Au decays. *Nucl. Instrum. Methods A284*, 393-398.

Collins, S.M., Pearce, A.K., Ferreira, K.M., Fenwick, A.J., Regan, P.H., Keightley, J.D., 2015a. Direct measurement of the half-life of ^{223}Ra . *Appl. Radiat. Isot.* 99, 46–53.

Collins, S. M., Pommé, S., Jerome, S. M., Ferreira, K. M., Regan, P. H., Pearce, A. K., 2015b. The half-life of ^{227}Th by direct and indirect measurements. *Appl. Radiat. Isot.* 104, 203-211.

Collins, S.M., Keightley, J.D., Ivanov, P., Arinc, A., Jerome, S.M., Fenwick, A.J., Pearce, A.K., 2018. The potential radio-immunotherapeutic α -emitter ^{227}Th – part II: absolute γ -ray emission intensities from the excited states of ^{223}Ra . *Appl. Radiat. Isot.*, In Press.

D'Agostino, G., Di Luzio, M., Mana, G., Oddone, M., 2017. A new low-uncertainty measurement of the ^{31}Si half-life. *Metrologia* 54, 410-416.

Dryák, P., Kovář, P., 2006. Experimental and MC Determination of HPGe Detector Efficiency within Energy Range from 40 keV up to 2754 keV for Measuring Geometry of Point Source in the Distance of 25 cm. *Appl. Radiat. Isot.* 64, 1346-1349.

Eurostandard CZ, <http://www.eurostandard.cz/Eurostandard-catalog-2011.pdf>.

Keightley, J.D., Pearce, A.K., Fenwick, A.F., Collins, S.M., Ferreira, K.M., Johansson, L., 2015. Standardisation of ^{223}Ra by liquid scintillation counting techniques and comparison with secondary measurements. *Appl. Radiat. Isot.* 95, 114–121.

Kellet, M. A., 2017. Private Communication.

Lépy, M.-C., Brondeau, L., Ménesguen, Y., Pierre, S., Riffaud, J., 2018. Consistency of photon emission intensities for efficiency calibration of gamma-ray spectrometers in the range from 20 keV to 80 keV. *Appl. Radiat. Isot.* 134, 131–136.

Mougeot, X., 2015. Reliability of usual assumptions in the calculation of β and ν spectra. *Phys. Rev. C* 91 (055504), 1-12.

MRTDosimetry project, 2016. <http://mrtdosimetry-empir.eu/>.

ORTEC, 2018. Gammavision. <https://www.ortec-online.com/products/application-software/gammavision>.

Piton, F., Lépy, M.-C., Bé, M.-M., Plagnard, J., 2000. Efficiency transfer and coincidence summing corrections for gamma-ray spectrometry. *Appl. Radiat. Isot.* 52, 791-795.

Pommé, S., 2015. The uncertainty of the half-life. *Metrologia* 52, S51-S65.

Ruellan, H., Lépy, M.-C., Etcheverry, M., Plagnard, J., Morel, J., 1996. A new spectra processing code applied to the analysis of ^{235}U and ^{238}U in the 60 to 200 keV energy range. *Nucl. Instrum. Methods A* 369, 651-656.

Seevinck, P. R., Seppenwoolde, J. H., de Wit, T. C., Nijsen, J. F., Beekman, F. J., van Het Schip, A. D., Bakker, C. J., 2007. Factors Affecting the Sensitivity and Detection Limits of MRI, CT, and SPECT for Multimodal Diagnostic and Therapeutic Agents. *Anti-Cancer Agents in Medicinal Chemistry*, 7(3), 317–334.

Smith, D., 1987. Some developments in the Cox-Isham theory of coincidence corrections, including the extension to the computer-discrimination method. *Appl. Radiat. Isot.*, 38, pp. 813-821.

Unterweger, M.P., Hoppes, D.D., Schima, F.J., 1992. New and revised half-life measurements results. *Nucl. Instrum. Meth. Phys. Res. A* 312, 349–352.

Unterweger, M.P., 2002. Half-life measurements at the National Institute of Standards and Technology. *Appl. Radiat. Isot.*, 56, 125-130.

Unterweger, M.P, Fitzgerald, R., 2014. Update of the NIST half-life results corrected for the ionization chamber source-holder. *Appl. Radiat. Isot.*, 87, 92-94.

Figure captions

Figure 1: Peak fitting in the X-ray emission range using Voigt functions.

Figure 2: Measured (\circ) and Monte Carlo calculated (\bullet) full-energy peak detection efficiencies in the case of the BEGe system at CMI.

Figure 3: Distribution of relative residuals associated to the fitting of the measurements obtained using a Vinten type 671 IC at LNHB.

Figure 4: Distribution of relative residuals associated to the fitting of the measurements obtained using a NaI(Tl) detector at LNHB.

Figure 5: Distribution of Relative residuals of the exponential fit of data measured with the GCX detector at CMI.

Figure 6: Residuals of the non-linear least squares fit (R_f) to the observed exponential decay rate (R_o) for the (a) ionisation chamber and (b) high purity germanium gamma-ray spectrometer at NPL.

Table captions

Table 1: Uncertainty budget related to $4\pi\beta\text{-}\gamma$ counting at LNHB.

Table 2: Uncertainty budget related to TDCR counting at LNHB.

Table 3: Experimental condition for photon spectrometry at LNHB. Measurements were performed with four sources, three of which were measured on each individual detector.

Table 4: Comparison of photon-emission intensities per 100 disintegrations obtained according to two geometry configurations at LNHB.

Table 5: Photon-emission intensities per 100 disintegrations in the low-energy range at LNHB.

Table 6: Summary of photon-emission intensities per 100 disintegrations for major lines in the decay of ^{166}Ho for each participating laboratory.

Table 7: Uncertainty budget for 80.6-keV photon-emission intensity measurement for each participating laboratory. In the CMI final data analysis, a discrepancy was found in the recorded weighing data related to the dilution. The effect of this potential mismatch on the dilution factor was included in the uncertainty budget (0.2%).

Table 8: Uncertainty budget related to $4\pi\beta\text{-}\gamma$ counting at CMI.

Table 9: Photon-emission intensities per 100 disintegrations for some lines in the decay of ^{166}Ho with 3 spectrometric systems at CMI.

Table 10: Uncertainty budget for the $4\pi(\text{LS})-\gamma$ digital coincidence counting performed at NPL.

Table 11: Uncertainty budget related to the half-life measurement of ^{166}Ho using a Vinten type 671 IC at LNHB.

Table 12: Uncertainty budget related to the half-life measurements based on γ -counting using a NaI(Tl) detector at LNHB.

Table 13: uncertainty budget related to the half-life measurements using a HPGe detector at CMI.

Table 14: Uncertainty components of the ionisation chamber and HPGe half-life determinations at NPL. Values provided after the uncertainty propagation using the formula derived by Pommé (2015). No medium frequency components were identified.

Table 15: ^{166}Ho half-life measurements at CMI, LNHB and NPL.

Figure 1

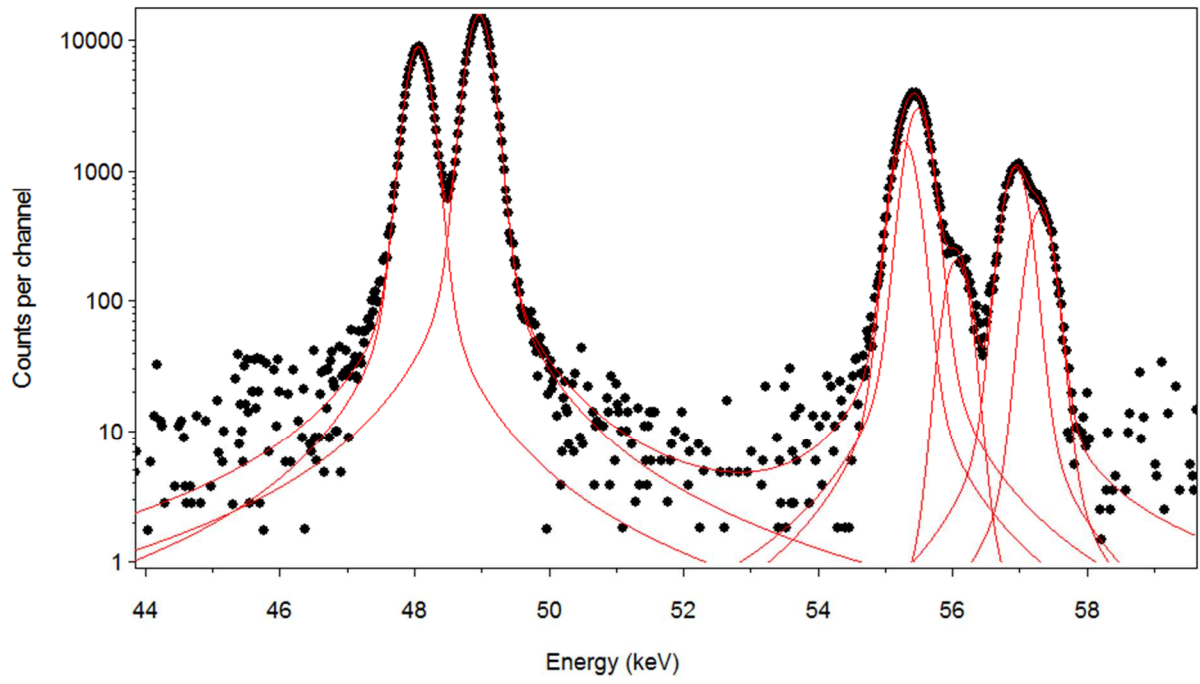


Figure 2

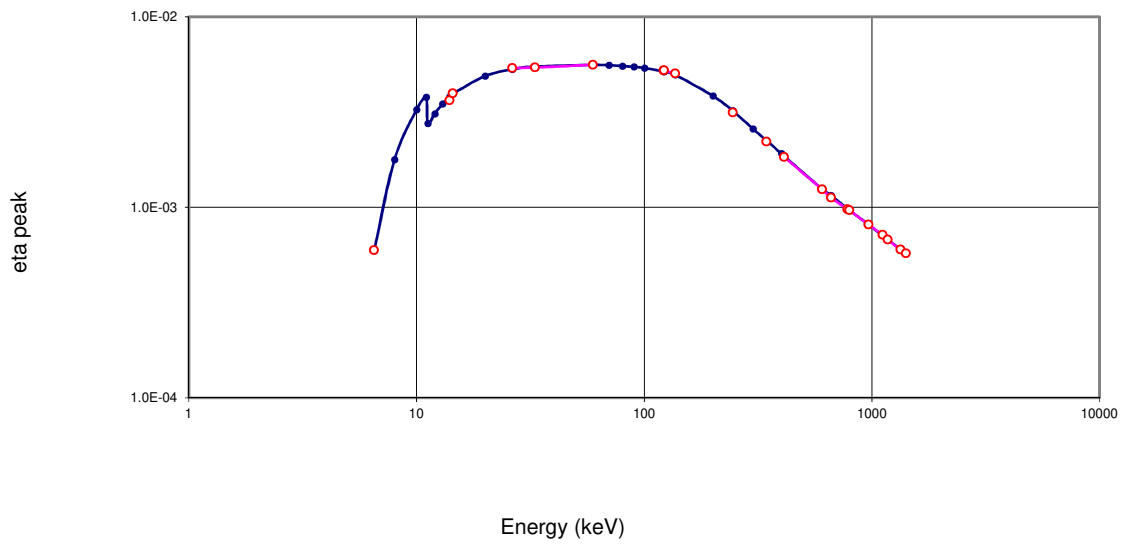


Figure 3

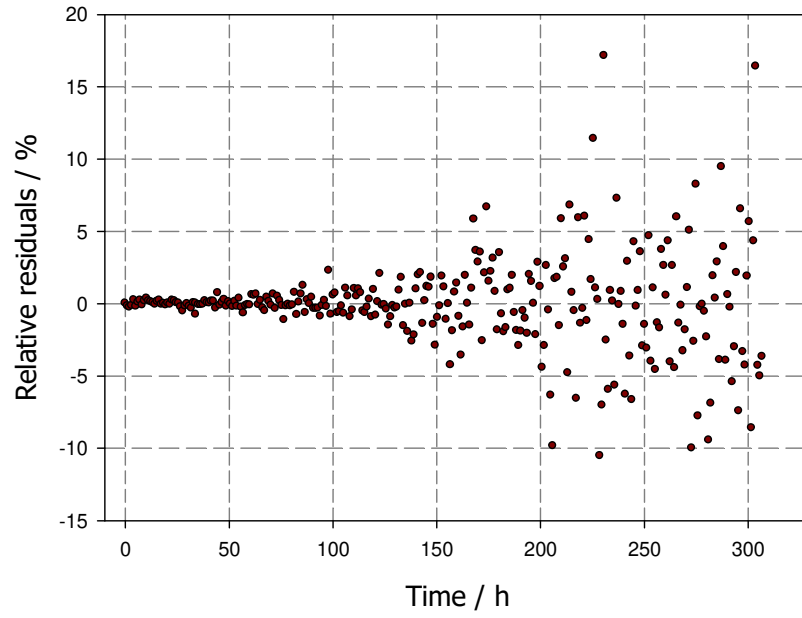


Figure 4

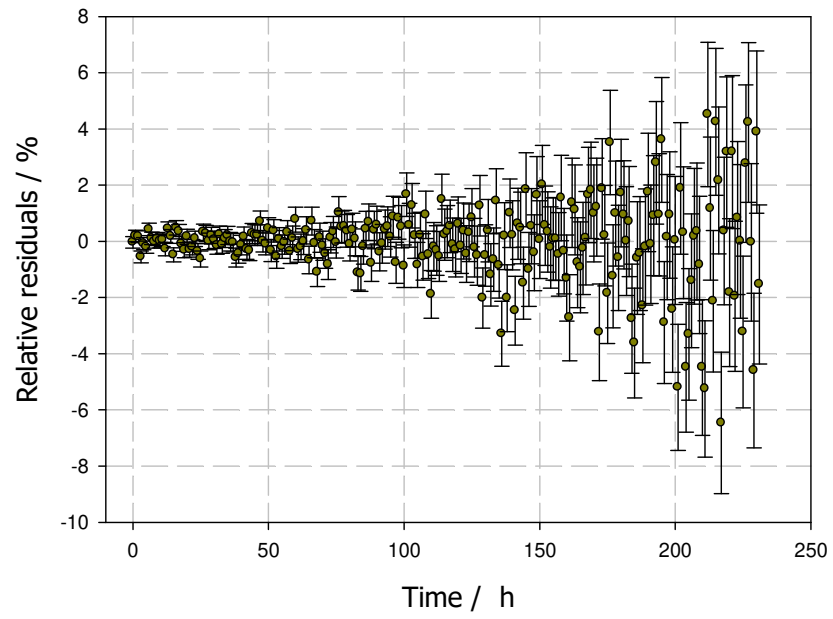


Figure 5

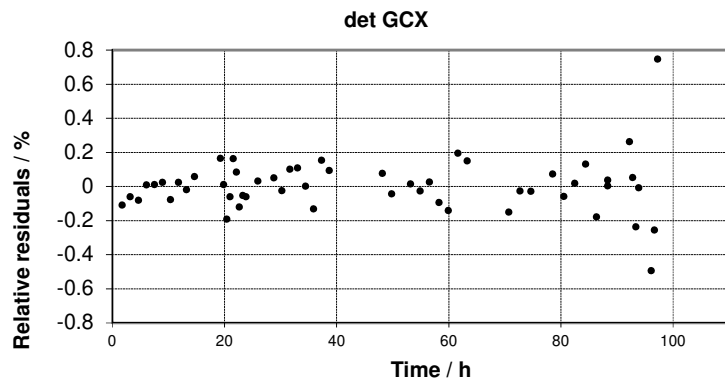


Figure 6

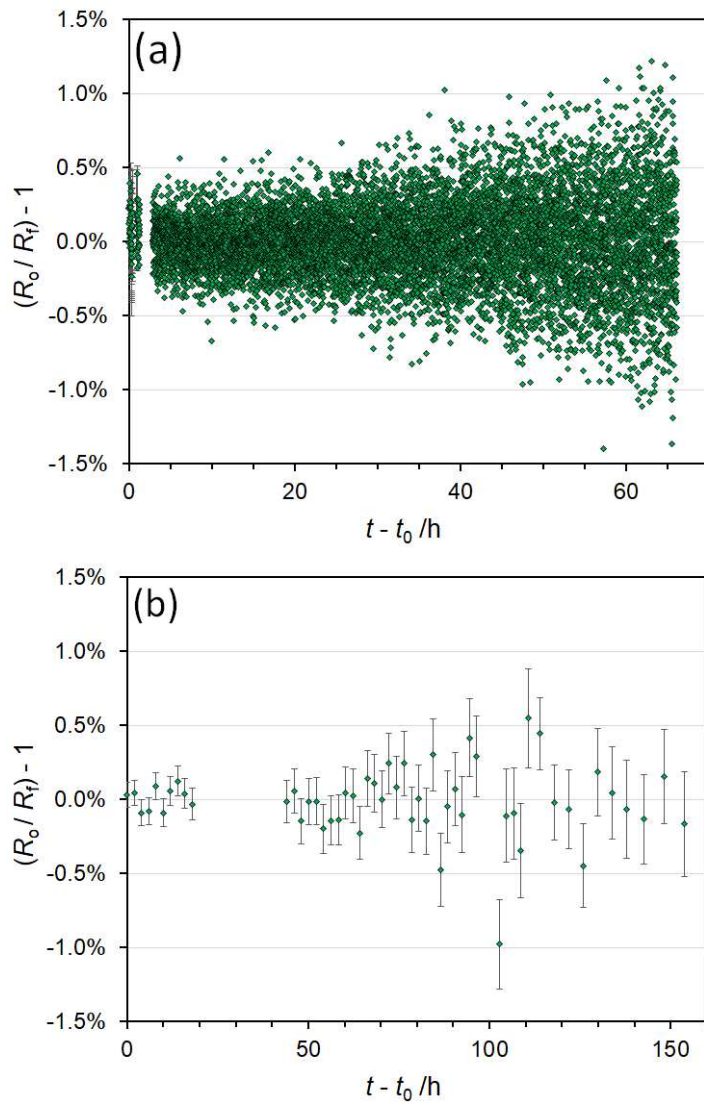


Table 1

Uncertainty component	Comments	$u(A_m) / \%$
Extrapolation technique and statistics	10 solid sources	0.08
Weighing	Gravimetric measurements (pycnometer method)	0.05
Live-time technique	MTR2 module	0.01
Background		0.02
Decay correction	Half-life of ^{166}Ho : 26.824 (30) h	0.1
Relative combined standard uncertainty		0.14

Table 2

Uncertainty component	Comments	$u(A_m) / \%$
Statistics	5 liquid sources	0.06
Weighing	Gravimetric measurements (pycnometer method)	0.05
Live-time technique	MAC3 module	0.01
Background		0.02
Decay correction	Half-life of ^{166}Ho : 26.824 (30) h	0.1
TDCR model		0.1
Relative combined standard uncertainty		0.16

Table 3

Detector	Crystal type	Calibration position	Measurement position	^{166}Ho sources
G8	Coaxial	10.7 cm	10.7 cm	3 sources (105, 66 and 101)
G9	Coaxial	10.3 cm	2.3 cm with 1.99 mm- thick lead	3 sources (356, 105 and 66)
GENIX	Planar	8 cm	8 cm	3 sources (66,101 and 105)

Table 4

Energy / keV	Measurement in the calibration conditions	Measurement at 2 cm with a screen
K alpha	8.26 (9)	
K beta	2.16 (2)	
80.57	6.60 (7)	6.59 (16)
674.24		0.0193 (8)
705.21		0.0134 (6)
785.78		0.0118 (6)
1379.45	0.896 (13)	0.891 (21)
1581.85	0.180 (4)	0.178 (4)
1661.61	0.114 (3)	0.114 (3)
1749.84		0.0259 (7)
1830.41		0.0080 (3)

Table 5

Energy / keV	LNHB results
K $_{\alpha 2}$: 48.22	3.048 (33)
K $_{\alpha 1}$: 49.13	5.33 (17)
K $_{\beta 1}$: 55.68	1.799 (20)
K $_{\beta 2}$: 57.21	0.575 (7)
80.57	6.62 (7)

Table 6

Energy / keV	Photon-emission intensities per 100 disintegrations			
	LNHB	CMI	NPL	DDEP (Bé et al., 2004)
K $_{\alpha 2}$ 48.22	3.048 (33)	2.944 (35)	2.944 (47)	2.91 (10)
K $_{\alpha 1}$ 49.13	5.33 (17)	5.217 (79)	5.257 (83)	5.16 (17)
K $_{\beta 1}$ 55.68	1.799 (20)	1.663 (20)	1.700 (26)	1.68 (6)
K $_{\beta 2}$ 57.21	0.575 (7)	0.436 (49)	0.4619 (69)	0.436 (18)
K $_{\alpha}$ total	8.37 (17)	–	–	8.07 (20)
K $_{\beta}$ total	2.37 (6)	–	–	2.116 (63)
80.57	6.61 (7)	6.636 (49)	6.618 (51)	6.55 (8)
184.41	–	–	0.001457 (70)	0.0015 (7)
674.24	0.0193 (8)	–	0.02142 (68)	0.0198 (17)
705.21	0.0134 (6)	–	0.01474 (65)	0.0146 (12)
785.78	0.0118 (6)	–	0.01306 (58)	0.0120 (3)
1379.45	0.896 (13)	0.904 (20)	0.9051 (69)	0.933 (35)
1581.85	0.180 (4)	0.180 (6)	0.1792 (24)	0.186 (4)
1661.61	0.114 (3)	0.1164 (41)	0.1157 (13)	0.118 (5)
1749,84	0.0259 (7)	–	0.02590 (48)	0.0272 (10)
1830,41	0.0080 (3)	–	0.00807 (26)	0.0081 (2)

Table 7

Uncertainty component	$u(I_\gamma) / \%$		
	CMI	LNHB	NPL
Statistics	0.41	0.05	0.032
Activity	0.16	0.15	0.43
FEP detection efficiency	0.5	1.0	0.57
FEP area	0.2	0.2	0.2
Pile-up correction	0.1	–	0.15
Decay correction (reference)	0.1	0.03	–
Decay correction (during counting)	–	0.07	–
Decay correction (reference + during counting)			0.03
Counting time	0.01	0.02	–
Dilution factor	0.2	–	–
Coincidence summing	0.01	0.002	0.05
Self-absorption	–	–	0.003
Weighing	–	0.013	0.02
Relative combined uncertainty	0.74	1.06	0.76

Table 8

Uncertainty component	Comments	$u(A_m) / \%$
Statistics	15 solid sources	0.06
Extrapolation technique		0.08
Weighing and dilution	Gravimetric measurements (pycnometer method)	0.1
Dead time		0.01
Background		0.02
Decay correction	Half-life of ^{166}Ho : 26.824 (30) h	0.08
Relative combined standard uncertainty		0.16

Table 9

Energy / keV	GC4018	GCX	BEGe
$K_{\alpha 2}$ 48.22	2.96 (6)	2.97 (6)	2.929 (35)
$K_{\alpha 1}$ 49.13	5.08 (10)	5.09 (12)	5.310 (64)
$K_{\beta 1}$ 55.68	1.635 (31)	1.656 (37)	1.676 (20)
$K_{\beta 2}$ 57.21	0.418 (10)	0.412 (16)	0.446 (6)
80.57	6.614 (49)	6.629 (49)	6.666 (49)
1379.45	0.915 (20)	0.906 (20)	0.885 (25)
1581.85	0.1814 (71)	0.1813 (59)	0.1773 (69)
1661.61	0.1162 (54)	0.1165 (41)	0.1164 (55)

Table 10

Uncertainty component	$u(A_0) / \%$
Standard deviation of mean	0.30
Dilution factor	0.15
Gravimetric	0.10
Background correction	0.050
Pulse pile-up in LS channel	0.020
Pulse pile-up in γ channel	0.020
Correction for accidental coincidences and finite resolving time	0.010
Decay correction	0.10
Range of fit for efficiency extrapolations	0.20
Choice of γ -gates/detectors	0.10
Impurities ($^{166\text{m}}\text{Ho}$)	negligible
Relative combined standard uncertainty	0.43

Table 11

Uncertainty component	Comments	$u(T_{1/2}) / \%$
High-frequency (statistics)	120 measurements	0.05
Medium-frequency (cyclic)		0.03
Low-frequency (drift)	Background variation	0.03
IC linearity		0.02
Relative combined standard uncertainty		0.068

Table 12

Uncertainty component	Comments	$u(T_{1/2}) / \%$
High-frequency (statistics)	230 measurements	0.05
Medium-frequency (cyclic)		0.03
Low-frequency (drift)	Background variation	0.05
Live-time and pile-ups		0.01
Relative combined standard uncertainty		0.08

Table 13

Uncertainty component	$u(T_{1/2}) / \%$
Statistics (fitting residuals)	0.0316
Pile-up	0.1
Counting time	0.001
Time corrections	0.01
Relative combined standard uncertainty	0.105

Table 14

Uncertainty component	$u(T_{1/2}) / \%$	
	IC	HPGe
High frequency		
Standard Deviation of residuals	0.0050	0.019
Low frequency		
Background correction	0.020	-
Detection efficiency stability	0.023	0.025
Dead time/ Pulse-pile up	-	0.075
Impurity	0.10	0.0050
Peak fitting	-	0.050
Relative combined standard uncertainty	0.10	0.10

Table 15

Radionuclide laboratory	Detection system	$T_{1/2}({}^{166}\text{Ho}) / \text{h}$
CMI	HPGe	26.828 (28)
LNHB	NaI(Tl)	26.818 (21)
	Ionization chamber	26.806 (18)
NPL	HPGe	26.800 (26)
	Ionization chamber	26.793 (27)
DDEP recommended value		26.795 (29)